Pure Appl. Chem., Vol. 75, No. 9, pp. 1287–1294, 2003.

Molecular and polymeric precursors to boron carbide nanofibers, nanocylinders, and nanoporous ceramics*

Mark J. Pender, Kersten M. Forsthoefel, and Larry G. Sneddon‡

Department of Chemistry, University of Pennsylvania, Philadelphia, PA 19104-6323, USA

Abstract: New decaborane-based, single-source molecular and polymeric precursors to boron carbide have been developed that enable the formation of boron carbide in processed forms, including nanofibers, nanocylinders, and nanoporous materials.

INTRODUCTION

The development of efficient methods for the production of complex structural and electronic materials in usable forms with controlled structures, orders, and porosities is one of the most challenging problems of modern solid-state chemistry and materials science. The chemical precursor approach, in which a polymeric or molecular precursor is first formed into the desired shape and then decomposed to the final solid-state material with retention of this shape, has been shown to be an important new route for producing many ceramics in a wide range of processed forms and sizes [1]. We report here our development of efficient routes to boron carbide nanostructured materials that has been made possible by the use of newly designed single-source boron carbide precursors in conjunction with nanoscale templating methods.

SINGLE-SOURCE BORON CARBIDE PRECURSORS

Boron carbide is a highly refractory material that is of great interest for both its structural and electronic properties [2]. Of particular importance are its high-temperature stability, high hardness, high cross-section for neutron capture, and excellent high-temperature thermoelectric properties [3]. This combination of properties gives rise to numerous applications, including uses as an abrasive wear-resistant material, ceramic armor, a neutron moderator in nuclear reactors, and, potentially, for power generation in deep space flight applications. Boron carbide is normally represented by a B_4C ($B_{12}C_3$) composition with a structure based on $B_{11}C$ icosahedra and C-B-C intericosahedral chains. However, single-phase boron carbides are also known with carbon concentrations ranging from 8.8 to 20 atom %. This range of concentrations is made possible by the substitution of boron and carbon atoms for one another within both the icosahedra and the three-atom chains.

While boron carbide powders are easily made by the direct reaction of the elements at high temperatures, new synthetic methods that allow the formation of pure boron carbide in processed forms are necessary for many potential applications. We have now achieved the syntheses of the decaborane-based polymeric and molecular single-source precursors, polyhexenyldecaborane and bis(decabo-

*Lecture presented at the XI[th] International Meeting on Boron Chemistry (IMEBORON XI), Moscow, Russia, 28 July–2 August 2002. Other presentations are published in this issue, pp. 1157–1355.

‡Corresponding author

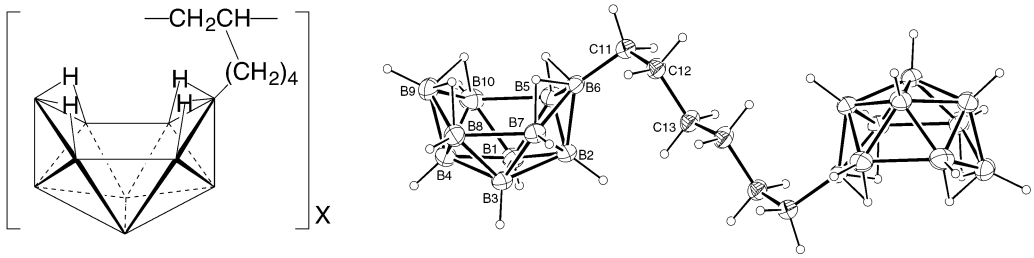

$[C_6H_{11}B_{10}H_{13}]_x$ 6,6'-$(CH_2)_6$-$(B_{10}H_{13})_2$

Fig. 1 Structures of new polymeric and molecular boron carbide precursors.

ranyl)hexane, shown in Fig. 1 and demonstrated that they can be used to provide boron carbide in processed forms.

The synthesis of the monomeric building block, 6-hexenyl-decaborane, that was needed for the construction of polyhexenyldecaborane was made possible by our discovery of a new metal-catalyzed method (eq. 1), involving the $Cp_2Ti(CO)_2$ catalyzed reaction of hexadiene with decaborane [4].

$$B_{10}H_{14} + CH_2 = CH\text{-}(CH_2)2\text{-}CH = CH_2 \xrightarrow{Cp_2Ti(CO)_2} \text{ 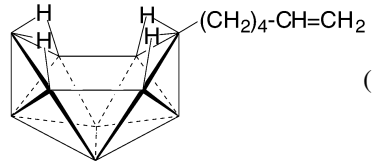 } \quad (1)$$

The 6-hexenyl-decaborane monomer is isolated in high yield (>90 %) as a stable liquid. Polymerization of the compound was then achieved [5] (eq. 2) by employing the $Cp_2ZrMe_2/B(C_6F_5)_3$ catalyst system [6] to yield white polymeric materials which are both air-stable for extended periods, and highly soluble in organic solvents.

$$6\text{-}(H_2C = CH\text{-}(CH_2)_4\text{-}B_{10}H_{13} \xrightarrow[B(C_6F_5)_3]{Cp_2ZrMe_2} [6\text{-}(\text{-}H_2CCH\text{-}(CH_2)_4)\text{-}B_{10}H_{13}]_X \quad (2)$$

The spectroscopic data for the polyhexenyldecaborane polymers are in excellent agreement with the inorganic/organic hybrid structure proposed in Fig. 1, consisting of a polyolefin-backbone with pendant decaboranes. The polymer T_gs are in the 50–60 °C, range and a thermogravimetric analysis (TGA) study showed that polymer decomposition does not begin until ~225 °C. Thus, the polymers are stable as melts. Also according to the TGA, the ceramic conversion reaction is essentially complete by 600 °C. The observed TGA (65 %) and bulk (60 %) ceramic yields are close to the theoretical ceramic yield of 68 % (eq. 3). X-ray diffraction (XRD) studies of the black, glassy ceramics obtained upon bulk pyrolyses of the polymer showed that samples heated to 1000 °C were amorphous, but those heated at 1250 °C (1 h) exhibited the onset of boron carbide crystallization.

$$2 \text{ 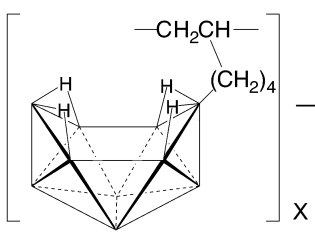 } \xrightarrow{1400°C} 5\ B_4C + C_7H_{16} + 16\ H_2 \quad (3)$$

Theoretical Ceramic Yield: 68 %
Observed Ceramic Yields: TGA: 65 %
Bulk: 60 %

Highly crystalline materials were obtained by heating the ceramics to 1850 °C. Elemental analyses of the resulting boron carbide ceramics derived from polyhexenyldecaborane indicate compositions in the range of B_4C. As discussed earlier, boron carbide can have compositions ranging from 8.8 to 20 atom % carbon and it has been shown that solid-state properties, such as hardness and thermoelectric efficiency, vary with the boron:carbon ratio. The ceramics derived from the polyhexenyldecaborane are thus on the "carbon-rich" side of the range of boron carbide compositions. However, by altering the boron to carbon ratio of the starting precursor, we have now also developed a new decaborane-based molecular precursor to "boron-rich" compositions.

The new precursor was synthesized by again employing the $Cp_2Ti(CO)_2$ catalyzed reaction of $B_{10}H_{14}$ with hexadiene, but the reactant ratios were altered to ensure hydroboration of both olefinic units. The 6,6′-$(CH_2)_6$-$(B_{10}H_{13})_2$ product is obtained by the reaction given in eq. 4 and is obtained as an off-white, air-stable solid in over 90 % isolated yields.

$$2B_{10}H_{14} + H_2C = CH\text{-}(CH_2)_2\text{-}CH = CH_2 \xrightarrow{Cp_2Ti(CO)_2} 6,6'\text{-}(CH_2)_6\text{-}(B_{10}H_{13})_2 \quad (4)$$

A TGA study of the 6,6′-$(CH_2)_6$-$(B_{10}H_{13})_2$ ceramic-conversion reaction showed that decomposition begins near 220 °C and is essentially complete by 400 °C. The XRD spectra of bulk powder samples of 6,6′-$(CH_2)_6$-$(B_{10}H_{13})_2$ pyrolyzed at 1000 °C (3h) indicated that they were amorphous, but powders heated at 1025 °C (3 h) exhibited the characteristic boron carbide diffraction pattern. Likewise, diffuse reflectance infrared (DRIFT) spectra of powders heated at 1025 °C (3 h) showed the major boron carbide bands. Consistent with the higher boron to carbon ratio (20:6) in 6,6′-$(CH_2)_6$-$(B_{10}H_{13})_2$ compared to that in polyhexenyldecaborane (10:6), the elemental analyses of the 1000 °C (B, 88.39; C, 11.45 %) and 1025 °C (B, 89.04; C, 10.76 %) ceramics obtained from 6,6′-$(CH_2)_6$-$(B_{10}H_{13})_2$ established $B_{7.7}C$ and $B_{8.3}C$ compositions, respectively. Thus, 6,6′-$(CH_2)_6$-$(B_{10}H_{13})_2$ is, in fact, an excellent precursor to "boron-rich" boron carbide.

Both the polyhexenyldecaborane polymer and the 6,6′-$(CH_2)_6$-$(B_{10}H_{13})_2$ compound appear to be ideal precursors for the syntheses of boron carbide materials in processed forms: (1) they are readily synthesized in large amounts using metal-catalyzed reactions; (2) they contain no other ceramic forming elements and have complementary boron to carbon ratios, thus yielding "carbon-rich" or "boron-rich" boron carbide compositions, respectively, upon pyrolysis; (3) they are stable as melts, thus allowing the use of melt-processing methods; and (4) upon pyrolysis, both precursors undergo a cross-linking reaction at relatively low temperatures (~220 °C) that retards loss of material by volatilization, thereby generating high ceramic and chemical yields.

SYNTHESIS OF BORON CARBIDE NANOSTRUCTURED MATERIALS

Nanoscale ceramic-fibers, -nanocylinders and -nanoporous structures, just like their well-known carbon counterparts, have a tremendous number of potential applications, including uses as quantum electronic materials, structural reinforcements, and ceramic membranes to be utilized for catalyst supports or gas separations [7]. Recently, Zhang et al. discussed the importance of nanoscale boron carbide materials and demonstrated the use of plasma-enhanced chemical vapor deposition to generate boron carbide nanowires and nanonecklaces [8]. Han et al. have also recently reported the formation of mixtures of crystalline boron carbide nanorods and boron-doped nanotubes upon the reaction of boron oxide vapor with carbon nanotubes [9]. Both of these methods are limited in their scales, and there is a clear need for the development of new methods for the more efficient formation of such materials.

Because of their processability and high ceramic and chemical yields, the single-source polyhexenyldecaborane and 6,6′-$(CH_2)_6$-$(B_{10}H_{13})_2$ precursors have now proven to be ideally suited for use in the generation of nanostructured materials. Some of our initial studies that utilize the unique properties of these precursors in conjunction with newly developed methods for nanofabrication are discussed below.

Nanofibers and nanocylinders

Porous alumina templates have recently been widely used to generate nanofibers from a variety of materials including polymers, carbon, metals, semiconductors, and ceramics [10]. This template method involves the absorption of a precursor material into the channels of the nanoporous alumina using either gas-phase or solution methods, conversion of the precursors to the final solid-state material by thermolytic or chemical reactions, and then dissolution of the alumina membrane to leave the free-standing fibers. In our work using these templating methods, we used alumina membranes having a thickness of 60 μm and a nominal pore size of ~250 nm as the templates. As outlined in Fig. 2, the membranes were immersed in liquid 6,6′-$(CH_2)_6$-$(B_{10}H_{13})_2$ at 140 °C until the membrane was saturated. The filled templates were then pyrolyzed to 1025 °C to yield a boron carbide-filled membrane. Immersing the sample in 48 % hydrofluoric acid for 36 h dissolved the alumina template. The fact that the fibers were not attacked by the HF treatment is in agreement with the chemical inertness of boron carbide.

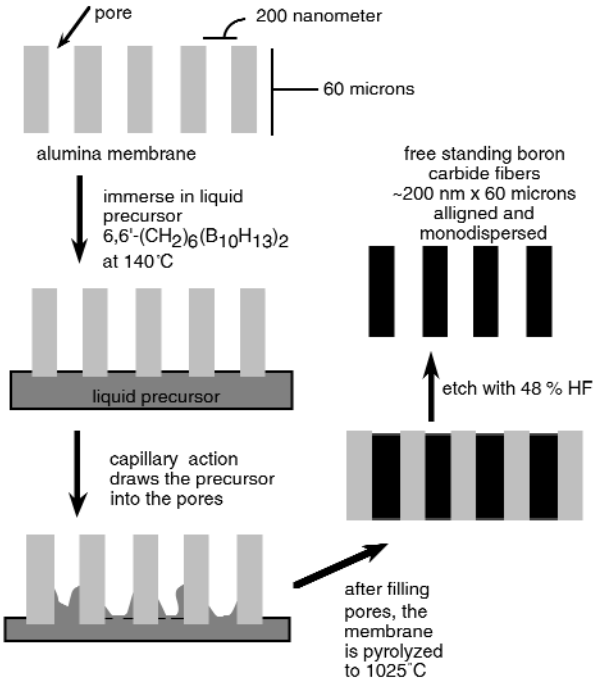

Fig. 2 Nanofiber synthesis.

The scanning electron microscopy (SEM) image in Fig. 3 shows a sample of nanofibers prepared as described above [11]. The fibers are uniform with an ~250 nm diameter and ~45 μm length. A thin layer of boron carbide was allowed to remain on one end of the fibers. This layer serves to hold the fibers in their parallel arrangement giving the highly aligned, brush-like configuration that is apparent in the figures. Thus, as has been previously noted, one of the advantages of the templating technique over other methods for generating nanofibers is its natural ability to produce aligned, monodispersed ensembles of nanofibers [10].

X-ray diffraction studies of these fibers showed that while the 1000 °C fibers are largely amorphous, the 1025 °C fibers are composed of crystalline boron carbide. In agreement with the XRD studies, analysis by transmission electron microscopy (TEM) confirmed that the nanofibers heated at 1000 °C (3 h) were amorphous, but those taken to 1025 °C (3 h) showed the onset of boron carbide crystallization.

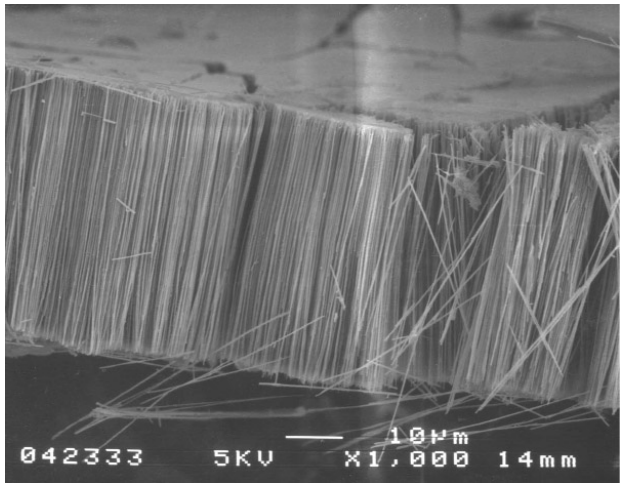

Fig. 3 SEM image of boron carbide nanofibers.

The methods described above provide efficient routes to nanofibers of boron carbide, as well as other nonoxide ceramics. We have also recently found that the porous alumina templating methods can be employed to produce nanocylindrical ceramic structures. Such hollow fiber structures are of great potential importance, since they could allow the efficient construction of multicomponent nanofibers. We have been able to produce such ceramic nanocylinders by a procedure similar to that reported by Martin et al. [10j] for the production of polymer nanotubes. Thus, in order to avoid completely filling the channels, a precursor solution, rather than the neat liquid precursor employed above for the nanofibers, is used to treat the membrane. For the production of boron carbide nanocylinders, a toluene solution of the polyhexenyldecaborane precursor is vacuum filtered through the template. The solvent is then completely evaporated to leave a thin precursor layer on the surfaces of the membrane. Pyrolysis of the coated membrane converts the precursor to a boron carbide coating.

Dissolution of the alumina membrane with HF then yields freestanding nanocylindrical boron carbide structures. The SEM image in Fig. 4 shows a side view of an ensemble of boron carbide nanocylinders that are ~50 µm long and ~250 nm in diameter and clearly shows the hollow cores of the

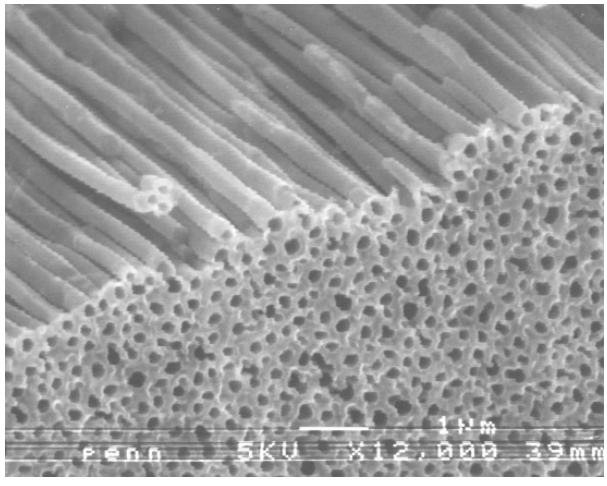

Fig. 4 SEM image of an end view of the boron carbide nanocylinders showing their hollow cores.

cylindrical structures. The inside diameter and wall thickness of the nanocylinders can be controlled by the solution concentration and/or number of membrane treatments.

In our initial studies of the syntheses of both nanofibers and nanocylinders, we have employed ~250 nm templates, but nanoporous alumina templates have been prepared with channels as small as 10–20 nm. We are now applying the methods that we developed in our initial work to generate and study these smaller dimension boron carbide fibers and nanocylinders.

Nanoporous boron carbide structures

The design of solids with ordered macroporosities has recently received great attention because of the possibility that such materials could potentially serve as photonic bandgap and optical stop-gap materials, as well as catalyst supports and gas separation membranes. Although methods for producing ordered porous materials with pore diameters less than 10 nm have been well developed, it has been only recently that the techniques for producing macroporous (>25 nm) materials with uniform pore sizes have been reported [12]. These methods generally involve the controlled growth of a matrix around an ordered array of macroscale templates. Silica spheres, latex beads, and triblock copolymers have each been employed as templates. Once the matrix structure is formed, the templates are then removed, by either chemical etching or thermal decomposition, to leave a macroporously ordered inorganic solid. For example, latex beads have been used as templates to construct, via sol-gel condensations, ordered macroporous arrays of titania, zirconia, and alumina. Other work employing the silica templates have yielded macroporous carbons. We have now used this templating technique to make macroporous nonoxide ceramic structures.

To generate macroporous boron carbide materials, we employed the method recently reported by Mallouk to generate a macro-ordered silica array [13]. Initially, a micro-emulsion of silica colliods was generated by controlled hydrolysis of tetraethoxysilane (TEOS). Then following the Mallouk method, these emulsions were dried, pressed, and sintered, as diagrammed in Fig. 5, to yield an array of ~50 nm

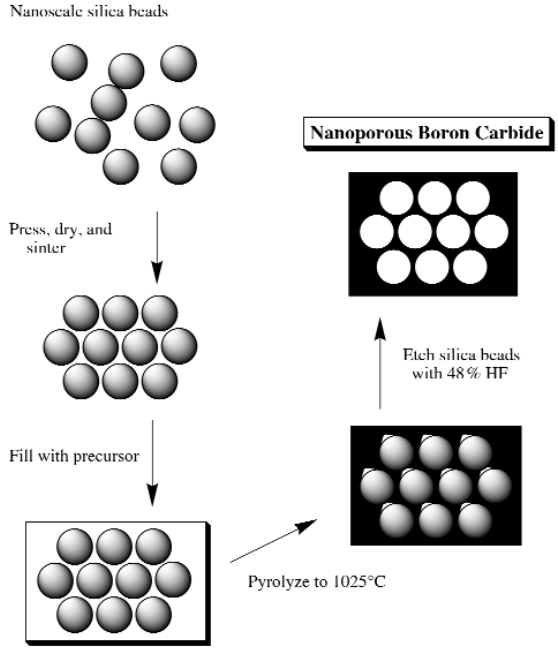

Fig. 5 Synthesis of nanoporous boron carbide.

diameter silica spheres. The open space in this framework was then filled with the boron carbide precursor 6,6′-$(CH_2)_6$-$(B_{10}H_{13})_2$ by immersion in a melt of the compound. Pyrolysis of the filled body to 1025 °C, then yielded a boron carbide matrix surrounding the silica spheres. The silica spheres were then etched from the matrix by treatment with 48 % HF to leave a "holey" boron carbide framework.

The TEM image in Fig. 6 indicates a boron carbide framework with reasonably ordered ~50 nm pores. We are now optimizing our procedures to both increase the ordering of the framework and achieve control of the hole size (through the use of different size silica beads) of the boron carbide framework.

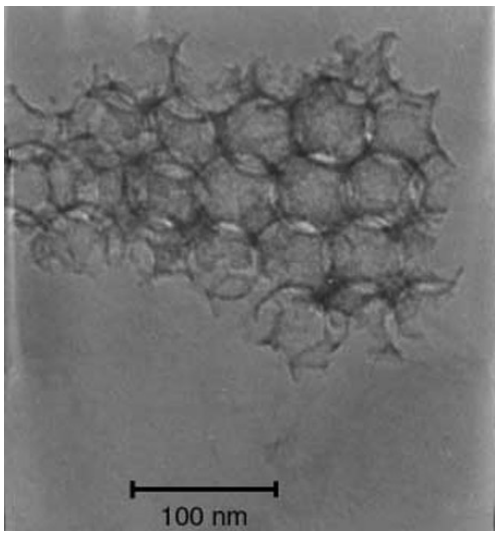

Fig. 6 TEM image of a nanoporous boron carbide framework.

In conclusion, the results discussed above have clearly demonstrated that nano-templating methods, in conjunction with appropriately designed molecular and polymeric single-source boron carbide precursors, allow the systematic generation of aligned, monodispersed ensembles of boron carbide nanofibers and nanocylinders, as well as ordered nanoporous materials. We are now investigating the structural and electronic properties of these materials, as well as the use of these template methods for the production a wide range of other nanostructured ceramics.

ACKNOWLEDGMENTS

We thank the Air Force Office of Scientific Research, USAF, under grant number F49620-01-1-0443 and the NSF-MRSEC program at the University of Pennsylvania for support of this work.

REFERENCES

1. K. J. Wynne and R. W. Rice. *Annu. Rev. Mater. Sci.* **14**, 297–334 (1984).
2. (a) F. Thevenot. *Key Eng. Materials* **56–57**, 59–88 (1991); (b) *Boron Rich Solids*, D. Emin, T. Aselage, C. L. Beckel, I. A. Howard, C. Wood (Eds.), AIP Conf. Proc 140, American Institute of Physics, New York (1986); (c) *Boron Rich Solids*, D. Emin, T. Aselage, A. C. Switendick, B. Morosin, C. L. Beckel (Eds.), AIP Conf. Proc 231, American Institute of Physics, New York (1991).

3. (a) C. Wood. In *Boron Rich Solids,* D. Emin, T. Aselage, C. L. Beckel, I. A. Howard, C. Wood (Eds.), pp. 362–372, AIP Conf. Proc 140, American Institute of Physics, New York (1986) and references therein; (b) T. L. Aselage, D. R. Tallant, J. H .Gieske, S. B. Van Deusen, R. G. Tissot. *The Physics and Chemistry of Carbides; Nitrides and Borides* **97** (1990).
4. M. J. Pender, P. J. Carroll, L. G. Sneddon. *J. Am. Chem. Soc.* **123**, 12222–12231 (2001).
5. M. J. Pender and L. G. Sneddon. *ACS Polym. Prepr.* **41**, 551–552 (2000).
6. X. Yang, C. L. Stern, T. J. Marks. *J. Am. Chem. Soc.* **116**, 10015–10031 (1994).
7. *Nanoscale Science, Engineering and Technology, Research Directions* report of the Basic Energy Sciences Nanoscience/Nanotechnology Group, U.S. Department of Energy, and references therein (1999).
8. (a) D. Zhang, B. G. Kempton, D. N. McIloy, Y. Geng, M. G. Norton. *Mat. Res. Soc. Proc.* **536**, 323–327 (1999); (b) D. Zhang, D. N. McIloy, Y. Geng, M. G. Norton. *Mat. Sci. Let.* **18**, 349–351 (1999).
9. W. Han, Y. Bando, K. Kurashima, T. Sato. *Chem. Phys. Lett.* **299**, 368–373 (1999).
10. See, for example: (a) C. R. Martin. *Science* **266**, 1961–1966 (1994); (b) C. R. Martin. *Acc. Chem. Res*. **28**, 61–68 (1995); (c) C. R. Martin. *Chem. Mater.* **8**, 1739–1746 (1996) and references therein; (d) B. B. Lakshmi, C. J. Patrissi, C. R. Martin. *Chem. Mater*. **9**, 2544–2550 (1997); (e) V. M. Cepak, J. C. Hulteen, G. Che, K. B. Jirage, B. B. Lakshmi, E. R. Fisher, C. R. Martin. *Chem. Mater.* **9**, 1065–1067 (1997); (f) G. Che, B. B. Lakshmi, C. R. Martin, E. R. Fisher, R. S. Ruoff. *Chem. Mater*. **10**, 260–267 (1998); (g) J. D. Klein, Herrick, II, D. Robert, D Palmer, M. J. Sailor. *Chem. Mater*. **5**, 902–904 (1993); (h) C. M. Zelenski, P. K. Dorhout. *J. Am. Chem. Soc.* **120**, 734–742 (1998); (i) Z. Zhang, D. Gekhtman, M. S. Dresselhaus, J. Ying. *Chem. Mater*. **11**, 1659–1665 (1999); (j) V. M. Cepak and C. R. Martin. *Chem. Mater.* **11**, 1363–1367 (1999).
11. M. J. Pender and L. G. Sneddon. *Chem. Mater.* **12**, 280–283 (2000).
12. A. Polman and P. Wiltzius. *Mater Res. Soc. Bull.* **26**, 608–646 (2001).
13. S. A. Johnson, P. J. Ollivier, T. E. Mallouk. *Science* **283**, 963–965 (1999).